DOI: 10.1002/adma.200502688

Transfer of Flexible Arrays of Vertically Aligned Carbon Nanofiber Electrodes to Temperature-Sensitive Substrates**

By *Benjamin L. Fletcher*, *Timothy E. McKnight*,* *Anatoli V. Melechko*, *Dale K. Hensley*, *Darrell K. Thomas*, *M. Nance Ericson*, and *Michael L. Simpson*

The unique physical, chemical, and mechanical properties of vertically aligned carbon nanotubes (VACNTs) and nanofibers (VACNFs) have led to their use in a variety of applications. VACNTs and VACNFs have demonstrated viability as field electron emitters,[1,2] electrochemical probes,[3,4] and biosensors.[5] These demonstrations have been enabled by the ability to deterministically synthesize vertically aligned nanostructures using catalytically directed plasma-enhanced chemical vapor deposition (PECVD) processes, where a carbonaceous source gas is decomposed and precipitated on catalyst nanoparticles at elevated temperatures. Catalyst activation in plasma requires substrate temperatures usually in the range 600–700 °C.[6–8] There have been several recent reports on carbon nanofibers grown at lower substrate temperatures.[9,10] However, it still remains an open question whether the graphitization quality of such nanofibers is sacrificed. The impact of low-temperature synthesis on the resultant structure's chemical, electrochemical, and mechanical properties also requires further exploration. In addition, the actual growth temperatures due to plasma heating could be considerably higher than those measured at the substrate heater.[11] These temperatures still impose restrictions on the types of substrates that can be used, with silicon and fused silica often being the substrates of choice owing to their compatibility with relatively high-temperature processes. Substrates sensitive to high temperatures, plasmas, or certain gases, including most polymers, glasses, and conventional microelectronics (i.e., complementary metal-oxide semiconductors, CMOSs), are degraded and sometimes destroyed by the harsh growth conditions of vertically aligned carbon nanostructures. As an alternative, in a recent report, carbon nanotubes encapsulated within an epoxy polymer were released from their growth substrate and aligned, using micromanipulators, on a receptor substrate in a low-temperature process.[12] This technique offers the advantage of preserving receptor substrates from the harsh growth conditions of carbon nanotubes. However, the spatial dimensions defined by the deterministic growth of nanotubes from photolithographically defined catalyst sites are lost. The necessity of realigning the encapsulated carbon nanotubes on the receptor substrate by micromanipulators also reduces the efficiency of the process.

We report on a method for growing VACNFs in a high-temperature (630 °C) direct-current PECVD process and subsequently transferring these nanofibers to new substrates. In brief, following high-temperature growth on silicon substrates, carbon nanofibers were partially embedded in a UV-cross-linked epoxy membrane and peeled from their original growth substrate. The membrane, featuring embedded high-aspect-ratio nanofibers, was then aligned and mated with an array of individually addressable contact pads. This process provides intact nanofibers that can be transferred to essentially any planar surface, including those that would otherwise be destroyed by the harsh conditions imposed on the substrate during nanofiber synthesis. Transferred carbon nanofibers were shown to retain their high-aspect-ratio morphology and their viability as electrodes, as demonstrated by electrochemical analysis and gold electrodeposition.

Nanofiber arrays were grown on silicon wafers from photolithographically defined nickel catalyst sites as previously described (Fig. 1C, process steps 1,2).[13] Following growth, nanofibers were inspected in a Hitachi 4700S scanning electron microscope at an acceleration voltage of 10 kV using a mixed-detector mode. Figure 1A presents a representative re-

[*] T. E. McKnight, B. L. Fletcher, Dr. A. V. Melechko, Dr. M. L. Simpson
Molecular Scale Engineering and Nanoscale Technologies Research Group
Oak Ridge National Laboratory
Bethel Valley Road, Oak Ridge, TN 37831 (USA)
E-mail: mcknightte@ornl.gov
T. E. McKnight, Dr. M. N. Ericson
Monolithic Systems Group, Oak Ridge National Laboratory
Bethel Valley Road, Oak Ridge, TN 37831 (USA)
B. L. Fletcher, Dr. M. L. Simpson
Materials Science and Engineering Department
University of Tennessee
434 Dougherty Hall, Knoxville, TN 37996 (USA)
Dr. A. V. Melechko, D. K. Hensley, D. K. Thomas, Dr. M. L. Simpson
Center for Nanophase Materials Sciences
Oak Ridge National Laboratory
Bethel Valley Road, Oak Ridge, TN 37831 (USA)

[**] The authors wish to thank P. H. Fleming and T. Subich for assistance with metal depositions. This work was supported in part by the National Institute for Biomedical Imaging and Bioengineering under assignment 1-R01EB000433-01 and through the Laboratory Directed Research and Development funding program of the Oak Ridge National Laboratory, which is managed for the U.S. Department of Energy by UT-Battelle, LLC. A. V. M. and M. L. S. acknowledge support from the Material Sciences and Engineering Division Program of the DOE Office of Science. A portion of this research was conducted at the Center for Nanophase Materials Sciences, which is sponsored at Oak Ridge National Laboratory by the Division of Scientific User Facilities, U.S. Department of Energy.

ADVANCED MATERIALS

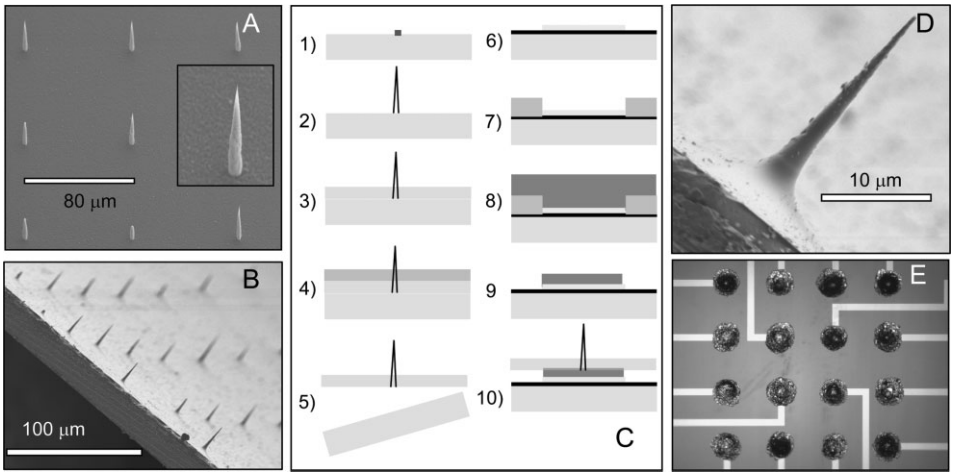

Figure 1. A) Scanning electron microscopy (SEM) image of an as-synthesized nanofiber array on its original growth substrate (silicon). Nanofibers in this array are spaced at an 80 μm pitch, and are approximately 40 μm tall. B,D) SEM images of a nanofiber membrane following peel-off from the original growth substrate. The membrane is composed of a 20 μm thick layer of SU-8 UV-crosslinkable epoxy. Nanofiber elements are buried in the membrane, with approximately 20 μm of the nanofiber emerging above the membrane surface. C) Process diagram with details described in the text. E) Gold-metallized interconnect device following patterned deposition of silver-loaded epoxy. Patterning of the silver-loaded epoxy was achieved by templating with a membrane of SU-8 UV-crosslinked photoresist that was peeled from the device after deposition of a thick epoxy film.

gion of the nanofibers. The bulk of nanofibers are approximately 40 μm tall, at a photolithographically defined pitch of 80 μm. Nanofibers which retained the nickel catalyst particle throughout growth featured tip diameters of approximately 100 nm (Fig. 1A, inset). Consistent with earlier reports,[14] nanofibers that lost the nickel catalyst owing to sputtering during growth were backetched, and are therefore significantly less sharp. An example of such a backetched nanofiber can be seen in the bottom center of Figure 1A. In addition to nanofiber synthesis, a thin carbon film was formed, shown in Figure 1B as a rough surface layer on the substrate beneath the nanofibers. Ammonia is typically added at a certain ratio to acetylene to prevent carbon-film formation.[15–17] By selecting slightly higher acetylene to ammonia flow ratios it is possible to control the formation of the carbon film, thereby tailoring the film to, in this case, provide a release layer for subsequent removal of the nanofibers–epoxy membrane.

After nanofiber synthesis, each wafer was spun with a UV-crosslinkable epoxy (SU-8) and flood exposed (Fig. 1C, process step 3). A protective layer of photoresist was then spun on and the wafer was diced into 4 mm squares (Fig. 1C, process step 4). Individual chips were soaked in acetone to remove the protective photoresist layer. At this time, the SU-8 membrane could be grabbed at the edge with sharp forceps and peeled from the underlying silicon substrate as intact, 4 mm × 4 mm films containing embedded VACNF elements (Fig. 1C, process step 5). These films could be further sized by slicing with a razor blade. In this study, the nanofibers embedded within the SU-8 membrane did not significantly impact our ability to remove the epoxy film from the original growth substrate, as the nanofibers themselves can be easily broken near the substrate. At their base, the nanofiber structure is similar to graphite, with graphene layers parallel to the substrate. Thus, the nanofibers are relatively weak here, as compared to the more-stable stacked-cone geometry found through the rest of their length.[17,18]

Figure 1B presents scanning electron microscopy (SEM) images of an SU-8 nanofiber membrane film upon removal from the underlying substrate. Owing to the presence of the passivating SU-8 dielectric, imaging was conducted at 1 kV to avoid charging. Images were captured using the Hitachi 4700S lower detector. Upon dicing, each membrane tended to curl slightly along one axis, which initiated the detachment of the film from the underlying silicon chip. This detachment was likely promoted by the presence of the amorphous carbon film on the surface of the silicon growth substrate. The amorphous carbon film on the bottom surface of the SU-8 membrane is visualized in Figure 1B as a bright region running the length of the bottom edge of the membrane. This film provides a large, conductive backplane of the membrane that later facilitates electronic connection to the nanofiber elements of the transferred membrane. In Figure 1D, nanofibers are seen to emerge approximately 20 μm above the SU-8 film. Close inspection of individual nanofiber elements in Figure 1D reveals that some SU-8 has spun up onto the fiber, resulting in curvature of the SU-8 layer around the base of each nanofiber, and likely some passivating SU-8 material on the sheath of each fiber.

A major advantage of using VACNFs is the ability to grow them in a deterministic manner, and to preserve this geometric patterning through the membrane-transfer process. The *x*- and *y*-positioning of catalyst dots, and hence the positioning of resulting nanofibers, is photolithographically defined. Tip, length, and width dimensions as well as chemical composition can also be controlled during nanofiber growth.[6,7,15,19–21] The SU-8 membrane acts as a semirigid

backbone and provides a means to preserve these features during the transfer process. In addition, the SU-8 membrane passivates all potentially active surfaces lying underneath. This limits electrical activity to the exposed portions of the carbon nanofibers.

To assess the ability to electrically address the nanofiber elements of the membrane, the membranes were transferred to arrays of individually addressable contact pads. These arrays were prepared from oxide-coated silicon wafers by defining contact pads and interconnect structures using photolithography. Following exposure and development, the defined structures were coated with evaporated gold, with the excess removed from unexposed regions using an acetone wash to lift off the photoresist and gold coating (Fig. 1C, process step 6). SU-8 was then spin-coated on the wafers and holes were patterned over the contact pads (Fig. 1C, process step 7). The wafer was diced using a wet dicing saw and stored for use. In preparation for mating, silver-loaded epoxy was smeared over the patterned SU-8 surface of each contact-pad device (Fig. 1C, process step 8). The SU-8 film was then peeled off using tweezers, leaving silver epoxy only on the exposed pads (Fig. 1C, process step 9). Figure 1E presents a microscopy image of the contact-pad-array device with patterned silver-loaded epoxy. Contact pads were regularly spaced at 320 μm intervals in a 4×4 matrix, forming an array of 16 pads. Electronic leads extend out from each, terminating in peripheral wirebonding pads provided for interconnection of the chip to a custom printed circuit board. The silver-loaded epoxy was patterned so that it was limited to the contact pads. This can provide a mechanism for controlling the number of carbon nanofibers addressed by each electronic lead.

To demonstrate electrical activity of the transferred nanofiber membranes, films sized to 1 mm × 1 mm–2 mm × 2 mm were mated by hand with the silver-loaded epoxy-patterned gold-contact-pad arrays and were heated to 65 °C for epoxy cure over a 1 h period (Fig. 1C, process step 10). The mated devices were then wire-bonded at the peripheral gold bonding pads to a custom printed circuit board. The wire-bonded devices were then maintained at 95 °C and carefully backfilled with epoxy (FDA2T, Tracon, Bedford, MA) such that the wire bonds and gold interconnect patterns were passivated, but the SU-8 nanofiber membrane was not. During this passivation, the height of the SU-8 membrane (approximately 20 μm) and its curvature along one axis was sufficient to dam the hot flowing epoxy at the membrane/interconnect interface such that the epoxy did not flow over the fibered membrane. The backfill epoxy was cured at 95 °C overnight.

Transferred nanofiber membranes were characterized using cyclic voltammetry (CV) with the quasireversible, outer-sphere analyte $Ru(NH_3)_6Cl_3$. Approximately 30 μL of 3 mM $Ru(NH_3)_6Cl_3$ in 300 mM KCl was placed on the nanofiber membrane. A 2.3 mm diameter reference electrode (Ag/AgCl (3 M KCl)) with a glass frit membrane was then placed in the solution. CV was conducted between 0 and –0.5 V at a scan rate of 500 mV s^{-1}. A resultant voltammogram is presented in Figure 2A.

The steady-state reduction current of $Ru(NH_3)_6^{3+}$ expected from an individually addressed nanofiber electrode was previously approximated[3] by assuming a semihemispherical electrode geometry with a surface area that is equivalent to the cylindrical or conical surface area of the nanofiber and employing the expression for semihemispherical microelectrodes:

$$i_{ss} = 2\pi r n F D C \quad (1)$$

where i_{ss} is the measured steady-state reduction current, r is the equivalent radius of a semihemispherical electrode with surface area equivalent to each nanofiber element of our multielectrode array, n is the number of electrons transferred in the redox process ($n = 1$ for $Ru(NH_3)_6^{+3}$), F is Faraday's constant (95 600 C mol^{-1}), D is the diffusion coefficient of $Ru(NH_3)_6^{+3}$ in 100 mM KCl (6.3×10^{-6} cm^2 s^{-1}), and C is the concentration (0.003 M). While more rigorous analysis of a cylindrical or conical nanofiber also includes non-steady-state contributions of the redox current, the bulk of the response

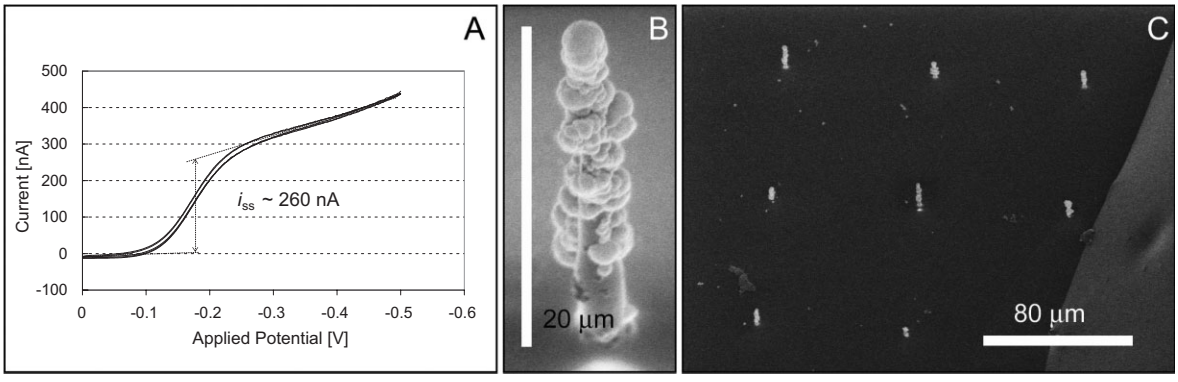

Figure 2. A) Cyclic voltammogram of a nanofiber membrane after transfer onto the gold-patterned interconnect device (as shown in Fig. 1E). The analyte is 3 mM $Ru(NH_3)_6^{2+/3+}$ in 300 mM KCl. Sweep rate is 500 mV s^{-1} and potential is recorded versus a Ag/AgCl (3 M KCl) reference. B) SEM image of a transferred nanofiber after deposition of gold to the electroactive surfaces. C) SEM image of the transferred nanofiber membrane after the deposition of gold. Gold deposition was limited to the emerging nanofiber electrodes. The SU-8 membrane and surrounding epoxy passivation effectively prevented electrodeposition from occurring upon the underlying gold interconnect device.

ADVANCED MATERIALS

can be described by this steady-state approximation.[21] This is observed in Figure 2A as a largely sigmoidal cyclic voltammogram, as first reported by Li et al. for an array of electrically addressed nanofiber electrodes.[22] The steady-state response of this voltammogram is approximately 260 nA. This magnitude is approximately 80× greater than that expected from a single nanofiber of the dimensions noted in Figure 1A. It has previously been reported that the electrochemical response of arrays of multiple nanofiber elements can be described as the algebraic sum of the individual nanofiber elements, provided the electrochemical boundary layers of elements do not overlap.[23] As such, we anticipate that the response seen in Figure 2A can be described approximately as:

$$i_{ss} = N[2\pi r n F D C] \quad (2)$$

where N is a scalar multiple equivalent to the total number of addressed nanofiber elements in the array. Based upon average surface areas of each nanofiber in Figure 1B, the scalar multiple describing the response of Figure 2A is approximately eighty, indicating that approximately eighty nanofibers were bulk addressed during the $Ru(NH_3)_6^{3+}$ characterization. In actuality, the membrane characterized in Figure 2A featured approximately twice this number of nanofibers, equivalent to a total membrane surface area of approximately 1 mm × 1mm.

The discrepancy between the estimated number of nanofibers and the actual count could be due in part to passivated regions on the emerging nanofiber tips. To test this hypothesis, gold electrodeposition was used to ascertain the physical location(s) of electrochemical activity (i.e., electron transfer) on transferred nanofiber membranes. Approximately 30 μL of a commercially available gold-plating solution (Orotherm HT Gold) was placed on the nanofiber membrane and a 2.3 mm diameter reference electrode (Ag/AgCl (3 M KCl)) with a glass frit membrane was then placed in the solution. Two cycles from 0 to –1.8 V to 0 were then performed at a scan rate of 500 mV s^{-1}. The array was rinsed in distilled water and imaged using SEM (Fig. 2B). Inspection revealed that gold deposition was limited to the emerging tips of the nanofibers, typically distributed over the top 80 % of the emerging nanofiber. The SU-8 membrane and backfill with FDA2T epoxy was effective at passivating the underlying interconnect pattern. The bases of most fibers were devoid of gold, likely due to the presence of passivating SU-8 spun up onto the fiber and crosslinked during the flood exposure associated with membrane fabrication. In addition, regions of the sidewalls of many fibers also were devoid of gold. Based on these observations and estimating that only approximately 50 % of the emerging nanofibers' surface area participated in electron transfer, the estimated and actual number of nanofibers addressed during acquisition of Figure 2A are in reasonable agreement.

We attempted additional processing of the nanofiber membrane to ascertain if individual addressability of the membrane nanofibers could be achieved. Up to this point, the amorphous carbon film on the original growth substrate was transferred with the nanofiber membrane, which resulted in bulk addressability of all nanofiber elements within the membrane. While this made interconnection to the nanofibers more convenient by providing a large backplane with which to interface, it also eliminated the potential for addressing individual nanofiber elements. As such, methods to eliminate transfer of this carbon film were developed. Prior to spinning the SU-8 photoresist membrane, the growth substrate was spun with a 7 μm thick layer of SPR220 CM 7.0 photoresist. This effectively provided a release layer between the SU-8 membrane and the underlying amorphous carbon film. Upon membrane peeling, however, the amorphous carbon film continued to transfer with the lifted membrane, even after acetone soaking, to remove the sandwiched SPR220 photoresist layer. Ultimately, in order to remove this film, nanofiber membranes were ultrasonicated for short periods (5 s each) until this amorphous carbon layer was broken and lost from the membrane. At this point, the SU-8 nanofiber membrane became transparent and much more flexible. SEM inspection revealed that the base of most nanofibers remained intact, providing an approximate 7 μm region of the nanofiber that emerged from the bottom of the SU-8 membrane. As with the bulk addressed membranes, these transparent membranes could be positioned over a silver-loaded epoxy pre-patterned interconnect substrate and electrically attached, with attachment likely facilitated by the 7 μm base emerging from the bottom of the SU-8 film. Following the attachment and backfill with passivating epoxy, the addressability of individual nanofibers was achieved as demonstrated by both $Ru(NH_3)_6Cl_3$ characterization (Fig. 3A) and gold electrodeposition (Fig. 3B). The former provided a steady-state response of approximately 0.65 nA for a singly addressed nanofiber, in reasonable agreement with expected values based on a shorter length being exposed from the SU-8 photoresist owing to the additional underlying 7 μm thick photoresist layer. To further confirm that only this nanofiber was addressed, the gold electrodeposition was conducted potentiostatically, clamping the electrode at –1.8 V versus Ag/AgCl (3 M KCl). Gold was electrodeposited for 30 s upon which the array was imaged with an optical microscope at 200×. Gold was then electrodeposited for an additional 30 s and the array was reinspected. Gold deposition was limited to one individual nanofiber element located on the silver-loaded epoxy bump-bonded interconnect.

In conclusion, carbon nanofibers were deterministically grown in a high-temperature (630 °C) PECVD process on a silicon substrate. The nanofibers were subsequently partially buried in SU-8 with approximately 40 % of their surface area exposed. The SU-8 layer and the imbedded carbon nanofibers were then peeled from the underlying growth substrate and transferred to an array of contact pads. The two structures were mated using patterned silver-loaded epoxy. The electrical viability of the transferred carbon nanofibers was tested in an electrochemical process, and a subsequent investigation of electrochemically active surfaces showed that activity was localized to the exposed surface area of the carbon nanofibers.

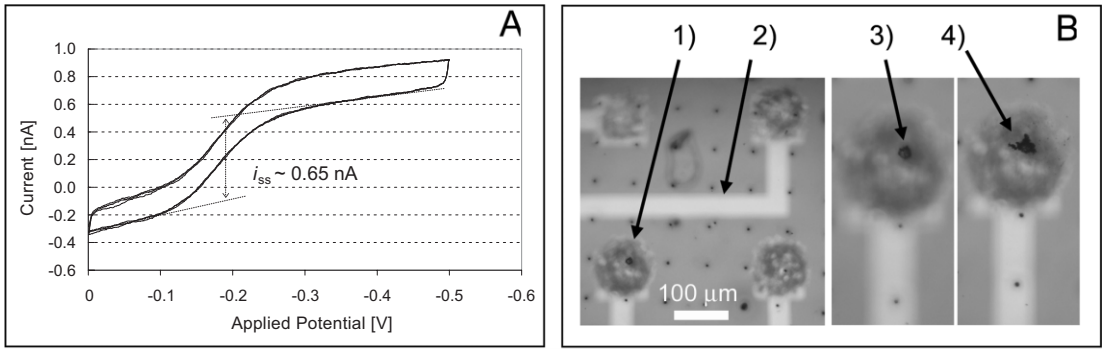

Figure 3. A) Cyclic voltammogram of an individually addressed nanofiber within a transferred membrane. The analyte is 3 mM $Ru(NH_3)_6^{2+/3+}$ in 300 mM KCl. Sweep rate is 500 mV s^{-1} and potential is recorded versus a Ag/AgCl (3 M KCl) reference. B) Optical microscopy images of the same individually addressed nanofiber following electrodeposition of gold. Labeled features include 1) silver-loaded epoxy bonding pads, 2) gold interconnects, 3) electrodeposited gold (30 s at –1.8 V) on an individually addressed carbon nanofiber electrode, and 4) the same carbon nanofiber electrode after further electrodeposition (30 s more at –1.8 V).

The resulting device shows promise as a three-dimensional, individually addressable nanoelectrode array that can be integrated with temperature-sensitive substrates such as CMOS circuitry. The transfer process also opens opportunities for transferring nanofiber electrodes onto nonplanar surfaces, which may have value for a variety of devices including biomedical applications such as retinal prostheses and peripheral-nerve interfacing. Furthermore, this transfer process can be extended for use with other fabricated structures or sensors, including carbon nanotubes, requiring synthesis temperatures not compatible with prefabricated substrates incorporating conventional integrated circuits or other temperature-sensitive materials.

Experimental

Gold Interconnect Device: Devices were prepared from prime grade 100 mm n-type silicon wafers with a 1000 nm thermal oxide deposited on the surface. These wafers were immersed in acetone, sonicated for 5 min, and washed with isopropyl alcohol to clean any organics and particulates from the surface. The wafers were then placed in a Yield Engineering System (YES) vacuum bake/vapor prime oven for dehydration and vapor deposition of hexamethyldisilazane (HMDS) priming agent. Shipley SPR955 CM 2.1 photoresist was spin-coated at 4000 rpm for 60 s and soft baked at 100 °C for 90 s. The contact-pad pattern was photolithographically defined under a Karl Suss MA6 Contact Aligner. After a post-exposure bake at 110 °C for 90 s, the pattern was developed in MicroChem MF-CD-26 photoresist developer. Residual photoresist was removed using oxygen plasma in a Trion Technologies Oracle reactive-ion-etch chamber. Layers of metal were then deposited using an electron-beam physical vapor deposition at 10^{-6} Torr (1 Torr = 133.32 Pa), 50 Å titanium for adhesion and 2000 Å gold for conduction. Excess metal was removed in an acetone lift-off leaving only the patterned metal. The wafer was heated to 180 °C to dehydrate the wafer. MicroChem SU-8 2015 was then spin-coated at 3000 rpm for 60 s and baked at 65 °C for 1 min then 95 °C for 2 min. Using the contact aligner, holes were patterned in the SU-8 photoresist over the contact pads. The post-exposure bake was carried out at 65 °C for 1 min then at 95 °C for 2 min and the pattern was developed in MicroChem SU-8 developer. The wafer was diced using a wet dicing saw (DiscoDad) into 1 cm × 1 cm devices and stored for use. In preparation for mating with transferred carbon nanofibers, silver-loaded epoxy (TRADUCT BA 2902, Tracon, Bedford, MA) was smeared over the patterned SU-8 surface of the contact-pad device. The SU-8 film was then peeled off using tweezers leaving silver epoxy only on the exposed pads. The resulting structure was inspected using a Mitutoyo WF semiconductor inspection scope at 200× magnification.

SU-8 Carbon Nanofiber Membrane: The SU-8 carbon nanofiber membranes were prepared on separate prime grade 100 mm n-type silicon wafers. Nanofiber arrays were grown from photolithographically defined nickel catalyst sites. In brief, the silicon wafers were vapor primed with HMDS. Wafers were then spun with Shipley SPR955 CM 0.7 photoresist at 2000 rpm for 60 s and soft baked at 90 °C for 90 s. Projection photolithography was then performed in a GCA Autostep 200 5× reduction stepper, providing an array of 600 nm holes in the photoresist at a pitch of 80 μm across the entire wafer. Wafers were post-exposure baked at 120 °C for 90 s and developed for 2 min in MF-CD-26. Development was inspected microscopically using a Zeiss Darkfield Inspection Microscope at 1000× magnification. A 30 s oxygen reactive-ion etch was then used to ash residual resist from the developed holes. Wafers were then metallized with 1000 Å of nickel using electron-gun physical vapor deposition. Excess metallization was lifted off by soaking the wafer in acetone for 1 h, followed by brief ultrasonication (5 s) and rinsing in a spray of acetone, isopropyl alcohol, and water. Individual wafers were then placed in a direct current PECVD chamber and pretreated with an ammonia-based etch to promote nickel particle nucleation from the patterned nickel film. The wafer was then heated to 630 °C and fiber synthesis was performed for 10 min with 60 sccm of NH_3 and 80 sccm of C_2H_2 at 20 Torr and 2 A of plasma current.

After nanofiber synthesis and inspection, each wafer was baked at 180 °C to dehydrate the surface, cooled to room temperature, and spun with SU-8 2015 at 2000 rpm for 60 s. The wafer was then softbaked at 65 °C for 2 min, and at 95 °C for 3 min. The wafer was then flood exposed for 15 s with the contact aligner, followed by a post-exposure bake at 65 °C for 2 min and at 95 °C for 3 min. A protective layer of Shipley SPR220 CM 7.0 photoresist was then spun on the wafer at 2000 rpm, followed by a softbake at 120 °C for 2 min. The wafer was then diced into 4 mm × 4 mm squares with the dicing saw. Individual chips were soaked in acetone for 5 min to remove the protective photoresist layer and sprayed with acetone, followed by isopropyl alcohol and water. At this time, the SU-8 layer on most chips could be grabbed at the edge with sharp forceps and peeled from the underlying silicon substrate as an intact 4 mm square film. This film could be further sized by slicing with a razor blade.

Received: December 15, 2005
Final version: March 27, 2006
Published online: June 8, 2006

[1] M. Katayama, K. Y. Lee, S. I. Honda, T. Hirao, K. Oura, *Jpn. J. Appl. Phys., Part 2* **2004**, *43*, L774.

[2] M. A. Guillorn, A. V. Melechko, V. I. Merkulov, E. D. Ellis, M. L. Simpson, D. H. Lowndes, *J. Vac. Sci. Technol., B* **2001**, *19*, 2598.

[3] M. A. Guillorn, T. E. McKnight, A. V. Melechko, V. I. Merkulov, P. F. Britt, D. W. Austin, D. H. Lowndes, M. L. Simpson, *J. Appl. Phys.* **2002**, *91*, 3824.

[4] J. Koehne, J. Li, A. M. Cassell, H. Chen, Q. Ye, H. T. Ng, J. Han, M. Meyyappan, *J. Mater. Chem.* **2004**, *14*, 676.

[5] S. E. Baker, K. Y. Tse, E. Hindin, B. M. Nichols, T. L. Clare, R. J. Hamers, *Chem. Mater.* **2005**, *17*, 4971.

[6] Z. F. Ren, Z. P. Huang, D. Z. Wang, J. G. Wen, J. W. Xu, J. H. Wang, L. E. Calvet, J. Chen, J. F. Klemic, M. A. Reed, *Appl. Phys. Lett.* **1999**, *75*, 1086.

[7] V. I. Merkulov, D. H. Lowndes, Y. Y. Wei, G. Eres, E. Voelkl, *Appl. Phys. Lett.* **2000**, *76*, 3555.

[8] K. Matthews, B. A. Cruden, B. Chen, M. Meyyappan, L. Delzeit, *J. Nanosci. Nanotechnol.* **2002**, *2*, 475.

[9] S. Hofmann, C. Ducati, J. Robertson, B. Kleinsorge, *Appl. Phys. Lett.* **2003**, *83*, 135.

[10] B. O. Boskovic, V. Stolojan, R. U. A. Khan, S. Haq, S. R. P. Silva, *Nat. Mater.* **2002**, *1*, 165.

[11] K. B. K. Teo, D. B. Hash, R. G. Lacerdo, N. L. Rupesinghe, M. S. Bell, S. H. Dalal, D. Bose, T. R. Govindan, B. A. Cruden, M. Chhowalla, G. A. J. Amaratunga, J. M. Meyyappan, W. I. Milne, *Nano Lett.* **2004**, *4*, 921.

[12] T. A. El-Aguizy, J. H. Jeong, Y. B. Jeon, W. Z. Li, Z. F. Ren, S. G. Kim, *Appl. Phys. Lett.* **2004**, *85*, 5995.

[13] A. V. Melechko, T. E. McKnight, D. K. Hensley, M. A. Guillorn, A. Y. Borisevich, V. I. Merkulov, D. H. Lowndes, M. L. Simpson, *Nanotechnology* **2003**, *14*, 1029.

[14] V. I. Merkulov, A. V. Melechko, M. A. Guillorn, D. H. Lowndes, M. L. Simpson, *Chem. Phys. Lett.* **2001**, *350*, 381.

[15] V. I. Merkulov, A. V. Melechko, M. A. Guillorn, D. H. Lowndes, M. L. Simpson, *Appl. Phys. Lett.* **2001**, *79*, 2970.

[16] K. B. Teo, M. Chhowala, G. A. J. Amaratunga, W. I. Milne, G. Pirio, P. Legagneux, F. Wyczisk, J. Olivier, D. Pribat, *J. Vac. Sci. Technol., B* **2002**, *20*, 116.

[17] A. V. Melechko, V. I. Merkulov, T. E. McKnight, M. A. Guillorn, K. L. Klein, D. H. Lowndes, M. L. Simpson, *J. Appl. Phys.* **2005**, *97*, 1.

[18] H. T. Cui, X. J. Yang, M. L. Simpson, D. H. Lowndes, M. Varela, *Appl. Phys. Lett.* **2004**, *84*, 4077.

[19] Y. H. Lin, F. Lu, Y. Tu, Z. F. Ren, *Nano Lett.* **2004**, *4*, 191.

[20] C. V. Nguyen, L. Delzeit, A. M. Cassell, J. Li, J. Han, M. Meyyappan, *Nano Lett.* **2002**, *2*, 1079.

[21] T. E. McKnight, A. V. Melechko, D. W. Austin, T. Sims, M. A. Guillorn, M. L. Simpson, *J. Phys. Chem. B* **2004**, *108*, 7115.

[22] J. Li, H. T. Ng, A. Cassell, W. Fan, H. Chen, Q. Ye, J. Koehne, J. Han, M. Meyyappan, *Nano Lett.* **2003**, *3*, 597.

[23] Y. Tu, Y. Lin, Z. F. Ren, *Nano Lett.* **2003**, *3*, 107.